



Partial photocatalytic oxidations of 3-pyridinemethanol and 3-picoline by TiO₂ prepared in HCl, HNO₃ and H₂SO₄ at different temperatures

Sıdıka Çetinkaya, Sedat Yurdakal *

Kimya Bölümü, Fen-Edebiyat Fakültesi, Afyon Kocatepe Üniversitesi, Ahmet Necdet Sezer Kampüsü, 03200 Afyonkarahisar, Turkey

ARTICLE INFO

This article is dedicated to the retirement and to the career of Prof. Leonardo Palmisano (University of Palermo, Italy) who devoted his life to Science and his students.

Keywords:

Photocatalysis
Home-prepared TiO₂
TiO₂ preparation in HCl, HNO₃ or H₂SO₄
Selective oxidation
3-Pyridinemethanol
3-Picoline
Vitamin B₃
3-Pyridinemethanol

ABSTRACT

Home prepared TiO₂ photocatalysts were prepared from TiCl₄ precursor in the absence and presence of HCl (1–6 M), HNO₃ (1 M) or H₂SO₄ (1 M) at room temperature (RT), 60 or 100 °C. The TiO₂ catalysts were characterised by XRD, BET, SEM and TGA techniques. TiO₂ catalyst could not form at low temperature (up to 60 °C) in the presence of H₂SO₄. Just rutile phase was obtained for all TiO₂ samples prepared at RT and 60 °C in HCl or HNO₃. At 100 °C mainly both brookite and rutile phases were obtained in the presence of HCl or HNO₃, whilst mainly anatase phase appeared in the presence of H₂SO₄. Nanorod structured TiO₂ was formed in the presence of 1 M HCl or HNO₃ at RT and 60 °C. The prepared TiO₂ catalysts were used for partial oxidation of 3-pyridinemethanol to 3-pyridinemethanal and vitamin B₃ in water under UVA irradiation. Moreover, photocatalytic oxidation of 3-picoline, precursor of 3-pyridinemethanol, was also performed, but much lower product selectivity values were obtained with respect to 3-pyridinemethanol oxidation. However, selective 3-picoline oxidation could be performed at pH 2 with low activity. Degussa P25 was used for comparison and almost all home prepared catalysts showed a higher selectivity, but they showed to be less active than Degussa P25. The high selectivity of the home prepared samples was not due to the type of TiO₂ phase, but mainly to the hydrophilicity of the TiO₂ surface which allowed desorption of valuable products instead of their over-oxidation.

1. Introduction

The researches on heterogeneous photocatalysis have been mainly addressed to elimination of harmful compounds in liquid and gas phases [1–5], hydrogen generation [6–10], CO₂ reduction [11–15], kinetics and mechanistic aspects of photocatalytic reactions [16–21], combination with photoelectrocatalysis [22–26], engineering aspects of photocatalytic processes [27–32] and production of commercial valuable compounds by efficient photocatalysts [33–40]. From these research topics, photocatalytic synthesis in water is gaining importance in recent years by an environmental point of view [33,37]. Photocatalytic synthesis reactions in which water is the solvent, oxygen from air is the oxidant and sun light is the irradiation source at ambient pressure and temperature could be considered as environmental friendly and they sometimes replace the traditional processes which are carried out in organic solvents in the presence of toxic oxidants at high pressure and temperature [35].

Organic solvents are generally used to perform the photocatalytic syntheses reactions because the reactions in water generally are not very

selective due to the presence of high concentrations of oxidant radical species [33,37]. However, some photocatalytic syntheses reactions in water have been successfully performed such as aromatic acid cyclization [41], oxidation of benzyl alcohols to the corresponding carbonyl derivatives [37,42], amines to imines [36], 5-(hydroxymethyl)-2-furaldehyde to 2,5 furandicarbaldehyde [43,44], piperonyl alcohol to piperonal [45], and glycerol mainly to 1,3 dihydroxyacetone [46–48].

Vitamin B₃, one of the main oxidation products of 3-picoline (3-methylpyridine) or 3-pyridinemethanol, is commonly used for alcoholism and prevention of pellagra disease [22,49]. Consequently, its annual production is high (ca. 66,000 ton in 2015) [50]. Vitamin B₃ is industrially produced by transformation of 3-picoline to 3-cyanopyridine, followed by a hydrolysis step, in the presence of vanadium oxide catalysts, oxygen and ammonia at high temperature (ca. 300 °C) [51–53]. In other words, the reaction conditions are not environmental friendly. Recently, different processes have been proposed to produce vitamin B₃ from 3-picoline oxidation by vanadia–titania catalysts or Cr_{(1-x)Al_xVO₄ and CrV_{(1-x)P_xO₄ mixed catalysts along with air at lower temperature (ca. 250 °C) [54,55].}}

* Corresponding author.

E-mail address: sedyurdakal@gmail.com (S. Yurdakal).

<https://doi.org/10.1016/j.cattod.2020.11.004>

Received 12 June 2020; Received in revised form 28 September 2020; Accepted 2 November 2020

Available online 25 November 2020

0920-5861/© 2020 Elsevier B.V. All rights reserved.

Only few research papers have been published on partial photocatalytic oxidation of 3-pyridinemethanol to corresponding aromatic aldehyde (3-pyridinemethanal) and aromatic acid (vitamin B₃) [35,49,53,56,57]. All these works were performed in water without adding any organic solvent [35,49,53,56,57]. Spasiano and co-workers performed this reaction by using pristine TiO₂ (anatase, Aldrich) and TiO₂-graphen-like photocatalysts in anaerobic medium, at low pH values (1–4) and in the presence of Cu²⁺ [49,53,56]. Yurdakal et al. investigated Pt loaded TiO₂ photocatalysts for selective oxidation of pyridinemethanols (*o*-, *m*-, *p*-) under UV, UV-vis and visible irradiations at pH 2–12 [35]. Poorly crystalline or well crystallized Pt loaded samples showed high selectivity in alkaline medium under UV or UV-vis irradiation. Only Pt loaded crystalline rutile sample showed significant activity only under Vis irradiation [35]. In addition, Sobahi and Amin prepared g-C₃N₄ nano-sheets decoration with Ag@TiO₂ nano-spheres for efficient vitamin B₃ synthesis from 3-pyridinemethanol under Vis irradiation [57].

Up to now, only a work on photocatalytic oxidation of 3-picoline has been published by Ohno and co-workers [58], in which methylpyridine isomers were oxidized to the corresponding aldehydes (pyridinecarboxaldehydes) in acetonitrile or in a mixed solution of acetonitrile and water by using different commercial TiO₂ powders.

TiO₂ is the most used photocatalyst because it is highly active, cheap, inert and resistant to photocorrosion [59,60].

In the present work, a systematic investigation was carried out for the first time on the 3-pyridinemethanol and 3-picoline activities and their selectivity to the products by using TiO₂ samples which presented different structures as they were prepared in HCl, HNO₃ or H₂SO₄ at different temperatures (RT, 60 or 100 °C). 3-Picoline photo-oxidation was performed differently from Ohno's work [58] in which the used TiO₂ catalysts were commercial, the solvent was not only water and the reaction was performed in anaerobic condition. The influence of the initial pH on the photocatalytic 3-picoline oxidation was also investigated in the present work. Previously, the effect of pH on the 3-pyridinemethanol oxidation has already been investigated by us [35].

2. Experimental part

2.1. Preparation of catalysts

The precursor solutions were obtained by slowly adding 20 mL of TiCl₄ (> 98 %, Merck) to 1000 mL water (1:50; TiCl₄:H₂O, v/v) [35], HCl (1, 3, 6 or 9 M), HNO₃ (1 M) or H₂SO₄ (1 M) solutions in a Pyrex bottle (1 L) under agitation. The Pyrex bottle was in an ace bath since the TiCl₄ hydrolysis is an exothermic reaction. After that, the bottles were sealed and maintained at room temperature (RT), 60 or 100 °C for a total aging time ranging from 6 to 27 days. In order to check the effect of more aging time, HP60–1 M HCl and HP60–1 M HNO₃ catalysts were maintained also for 108 days (named as HP60–1 M HClb and HP60–1 M HNO₃b, respectively). Then, the precipitated catalysts were dialysed by using a polymeric membrane several times with deionised water until reaching neutral pH, and were dried at 60 °C by a rotary evaporator (Heidolph, model M) working at 100 rpm. However, the samples prepared at RT were dried also at RT. The catalysts were named as “HPX-yM-acid name” in which HP means “home prepared”, “X” indicates the aging temperature and “y” the acid concentration.

2.2. Characterization

XRD patterns of the powdered TiO₂ samples were recorded by Bruker D8 Advance diffractometer by using the Cu K α radiation and a 2 θ scan rate of 1.281°/min. The crystallinity of the rutile, anatase and brookite phases present in home prepared samples was evaluated by the procedure reported below [61,62]. For this aim, XRD diffractograms were recorded for a mixture of TiO₂ and completely crystalline CaF₂ (1:1, w/w). The equations (Eq. 1–3) were shown below and the absolute

crystallinity of the phases was calculated from the ratio between the FWHM of the XRD (111) peak of CaF₂ with each phase (anatase (101), rutile (110) or brookite (121)).

$$\text{Crystallinity of TiO}_2 \text{ rutile} = \frac{1}{0.98} \times \frac{\text{FWHM CaF}_2 (111)}{\text{FWHM rutile (110)}} \times 100\% \quad (1)$$

$$\text{Crystallinity of TiO}_2 \text{ anatase} = \frac{1}{1.15} \times \frac{\text{FWHM CaF}_2 (111)}{\text{FWHM anatase (101)}} \times 100\% \quad (2)$$

$$\text{Crystallinity of TiO}_2 \text{ brookite} = \frac{1}{1.04} \times \frac{\text{FWHM CaF}_2 (111)}{\text{FWHM brookite (121)}} \times 100\% \quad (3)$$

Thermogravimetric analyses (TGA) of the catalysts were performed by using a Shimadzu equipment (model TG60H) in nitrogen atmosphere. The heating rate was 10 °C min⁻¹. The used catalyst amount was ca. 12 mg in an open Pt crucible.

BET specific surface areas were measured by the multi-point BET method using a Micromeritics (Gemini 2360 model) apparatus. Before the measurement, the TiO₂ samples were outgassed for 3 h at 250 °C. Scanning electron microscopy (SEM) images of TiO₂ powders were obtained by using FEI microscope (NanoSEM 650 model). The samples were covered by a gold thin film before the SEM analysis.

2.3. Setup and procedure of photoreactivity experiments

Figure S1 shows the photo of photocatalytic system used for the runs, the lamps and the spectra of the lamps. A cylindrical beaker (250 mL) containing 150 mL of aqueous suspension was used as photoreactor. Four fluorescent lamps (Philips, 8 W) were used for UVA source irradiating at 365 nm as the maximum wavelength. These lamps were positioned at a distance of 6.8 cm from the top of the suspension and they were parallel each other. The average value of the radiation energy impinging on the suspensions, measured by using a radiometer (Delta Ohm, DO9721), was 21 W m⁻² in the 315–400 nm range. Preliminary reactivity tests, carried out with both substrates and their corresponding products, showed that the contemporary presence of catalyst, radiation and oxygen was necessary for the occurrence of the substrate oxidation.

The substrate initial concentration was 0.50 mM and the used catalyst amount was 0.20 g L⁻¹. The suspension pH was adjusted by using 0.1 M HCl or NaOH solutions. Before switching on the lamp, the suspension was stirred for 30 min in order to reach the thermodynamic and adsorption-desorption equilibria. The photoreactivity experiments were performed at room temperature (ca. 25 °C). The contact of the suspension with the atmosphere guaranteed that the aqueous suspension was saturated by oxygen during the course of the run. During the photocatalytic runs, continuously stirred, the samples of the suspension were withdrawn at fixed time intervals and filtered immediately with a hydrophilic membrane (0.45 μ m, HA, Millipore) before being analysed by HPLC and TOC as described below.

2.4. Analytical techniques

The qualitative and quantitative determination of withdrawn samples from reacting suspension were performed by using HPLC instrument (Shimadzu, Prominence LC-20A model and SPD-M20A Photodiode Array Detector), equipped with a Thermo Scientific Synchronis C18 column (particle size: 5 μ m, length: 25 cm, inside diameter: 4.6 mm) at 313 K. Retention times and UV-vis spectra of the compounds were compared with those of standards (Sigma-Aldrich, \geq 98 %). The eluent consisted of 40 % methanol and 60 % deionised water, and the flow rate was 0.4 cm³ min⁻¹. TOC analyses were performed by using a Total Organic Carbon analyser (Shimadzu, TOC-LCPN model) to evaluate the mineralized CO₂ amount of substrates. CO₂ selectivity values were divided by 6 for stoichiometric normalization. The selectivity and conversion values were calculated as below:

Table 1

Aging time for TiO₂ formation, crystalline phase and its crystallinity, primary particle size, agglomerate sizes, BET specific surface area, pore volume and pore size values of home prepared and Degussa P25 TiO₂ catalysts. A: Anatase; B: Brookite; R: Rutile; W: width; L: length.

Catalyst	Aging time (day)	Phase and crystallinity (%)	Primary particle size (nm)	Agglomerate size (nm)	Specific surface area (m ² g ⁻¹)	Pore volume (cm ³ g)	Pore size (nm)
Degussa P25		A, R	18:20 (A:R)	25	63.5	0.195	10.4
HPRT	6	R (34 %)	7.0	20–60 (W- L)	146	0.227	7.54
HPRT-1 M HCl	27	R (21 %)	13.3	35–130 (W- L)	144	0.470	18.9
HPRT-1 M HCl _b	108	R (17 %)	17.4		113	0.664	22.0
HPRT-1 M HNO ₃	27	R (20 %)	11.3	25–150 (W- L)	117	0.710	25.8
HPRT-1 M HNO ₃ _b	108	R (21 %)	13.7		80.4	0.423	17.0
HPRT-1 M H ₂ SO ₄	It could not obtained significantly after 2 years of aging time						
HP60	6	R (28 %)	14.4	30	307	1.07	12.0
HP60–1 M HCl	6	R (23 %)	14.0	25–200 (W- L)	90.2	0.520	21.9
HP60–1 M HNO ₃	6	R (24 %)	13.6	30–250 (W- L)	80.2	0.366	15.3
HP60–1 M H ₂ SO ₄	It could not obtained significantly after 10 days of aging time						
HP100	6	R (38 %), B (22 %), A,	7.41;17.84 (A;R)	25	116	0.250	6.43
HP100–1 M HCl	6	B (32 %), R (33 %), A	12.1; 18.4 (A;R)	25	91.3	0.448	15.8
HP100–3 M HCl	6	B (39 %), A, R	10.2 (A and B))	35	139	0.592	19.0
HP100–6 M HCl	6	R	25.6	30	7.92	0.0157	7.7
HP100–9 M HCl	It could not obtained significantly after 6 days of aging time						
HP100–1 M HNO ₃	6	R (35 %), B (57 %), A	10.8;13.9 (A;R)	25	105	0.415	10.9
HP100–1 M H ₂ SO ₄	6	A (25 %)	12.5	30	146	0.208	9.9

$$\text{selectivity (\%)} = \frac{(\text{produced product amount, mmol})}{(\text{converted substrate amount, mmol})} \times 100$$

$$\text{conversion (\%)} = \frac{(\text{reacted substrate amount, mmol})}{(\text{initial substrate amount, mmol})} \times 100$$

3. Results and discussion

3.1. Characterization part

Home prepared (HP) TiO₂ catalysts were obtained in the presence of different acids (HCl, HNO₃ or H₂SO₄) at different temperatures (room temperature (RT), 60 or 100 °C). Some catalysts were prepared without using any acid at different temperatures (HPRT, HP60 and HP100). Depending on the precursor condition (type and concentration of the used acid and aging temperature), different aging times were needed for TiO₂ formation. No TiO₂ catalyst was obtained in the presence of 1 M H₂SO₄ at RT for very long time (more than 2 years) or maintaining the temperature at 60 °C for 10 days. Nevertheless, TiO₂ was obtained at 100 °C, a moderately high temperature, in the presence of 1 M H₂SO₄. At RT and in the presence of 1 M HCl or 1 M HNO₃, much long aging times (27 vs 6 days in their absence) were necessary for observing formation of TiO₂ (see Table 1). In addition, in the presence of 9 M HCl at 100 °C, no TiO₂ nanoparticles were formed. These results show that the acids (especially H₂SO₄ and at RT) inhibit the TiO₂ formation from the used TiCl₄ precursor.

Fig. 1 shows XRD patterns of the prepared TiO₂ catalysts and Degussa P25. The analyses to evaluate the crystallinity of the catalysts were carried out with the same mass of CaF₂. The analyses details were reported in the Experimental section. The XRD peaks at 2 θ = 27.5°, 36.5°, 41.0°, 54.1°, 56.5° can be attributed to the rutile TiO₂, those at 2 θ = 25.58°, 38.08°, 48.08°, 54.58° to anatase TiO₂, while those at 2 θ = 25.3°, 30.9°, 46.3°, 55.8° to brookite TiO₂ [43]. Degussa P25, used for the sake of comparison, shows anatase (A) and rutile (R) phases (ca. 80 % A and 20 % R). All home prepared samples were poorly crystallized, and presented low and broad XRD lines with respect to those of the crystalline CaF₂, due to the low preparation temperatures (up to 100 °C)

used. The TiO₂ catalysts prepared at RT and 60 °C were in the rutile phase, whilst different TiO₂ phases were obtained at 100 °C, depending on the type and concentration of the acid used. In the absence of used acid mainly anatase and rutile phases were found, in the presence of 1 M H₂SO₄ virtually only anatase, and in the presence of 1 M HCl or HNO₃ mainly rutile and brookite phases. In the last event, both HCl and HNO₃ showed similar behaviour, different from H₂SO₄. In the presence of 3 M HCl, high brookite content was achieved, while in the 6 M HCl (extreme condition) just rutile phase was produced.

Table 1 reports the aging time needed to obtain TiO₂, type of crystalline phase, the phase crystallinity, primary particle size, agglomerate size, BET specific surface area, pore volume and pore size values of all TiO₂ catalysts. Figure S2 shows some adsorption-desorption curves of TiO₂ samples, and it can be noticed that Type II adsorption isotherms were obtained [63]. All primary particle size values, determined by Scherrer equation, were in the range of 7.0–26 nm. By increasing the aging time from 27 to 108 days, primary particle sizes increased (i.e. 13.3 vs 17.4 nm for HPRT-1 M HCl) due to the longer time that induced the growth of the particles. Consequently, the BET surface area values decreased (i.e. 144 vs 113 m² g⁻¹) for HPRT-1 M HCl). The pores of all TiO₂ samples can be classified as mesopores as their size ranged between ca. 6 and 26 nm. HP100-6 M HCl sample, prepared under drastic experimental condition, showed very special properties; its BET specific surface area, the pore volume and the pore size values were very low. Indeed, with the exception of this sample, all home prepared samples have higher surface area than Degussa P25. HP60 showed to have the highest BET specific surface area (307 m² g⁻¹). The samples appeared poorly crystallized and the crystallinity generally increased by increasing the preparation temperature from RT to 100 °C. For instance, rutile crystallinity of HPRT-1 M HCl, HP60-1 M HCl and HP100-1 M HCl were 21, 23 and 33 %, respectively. We think that the use of the FWHM values can not be always satisfactorily, especially when they were low due to too small peaks. For example, the calculated crystallinity of trace rutile peak of HP100-3 M-HCl by using Eq. 1 resulted to be 67 %! Therefore, we always considered significant peaks and the calculated value of HP100-3 MHCl was not reported in the Table.

Fig. 2 and S3 show SEM micrographs of home prepared and Degussa

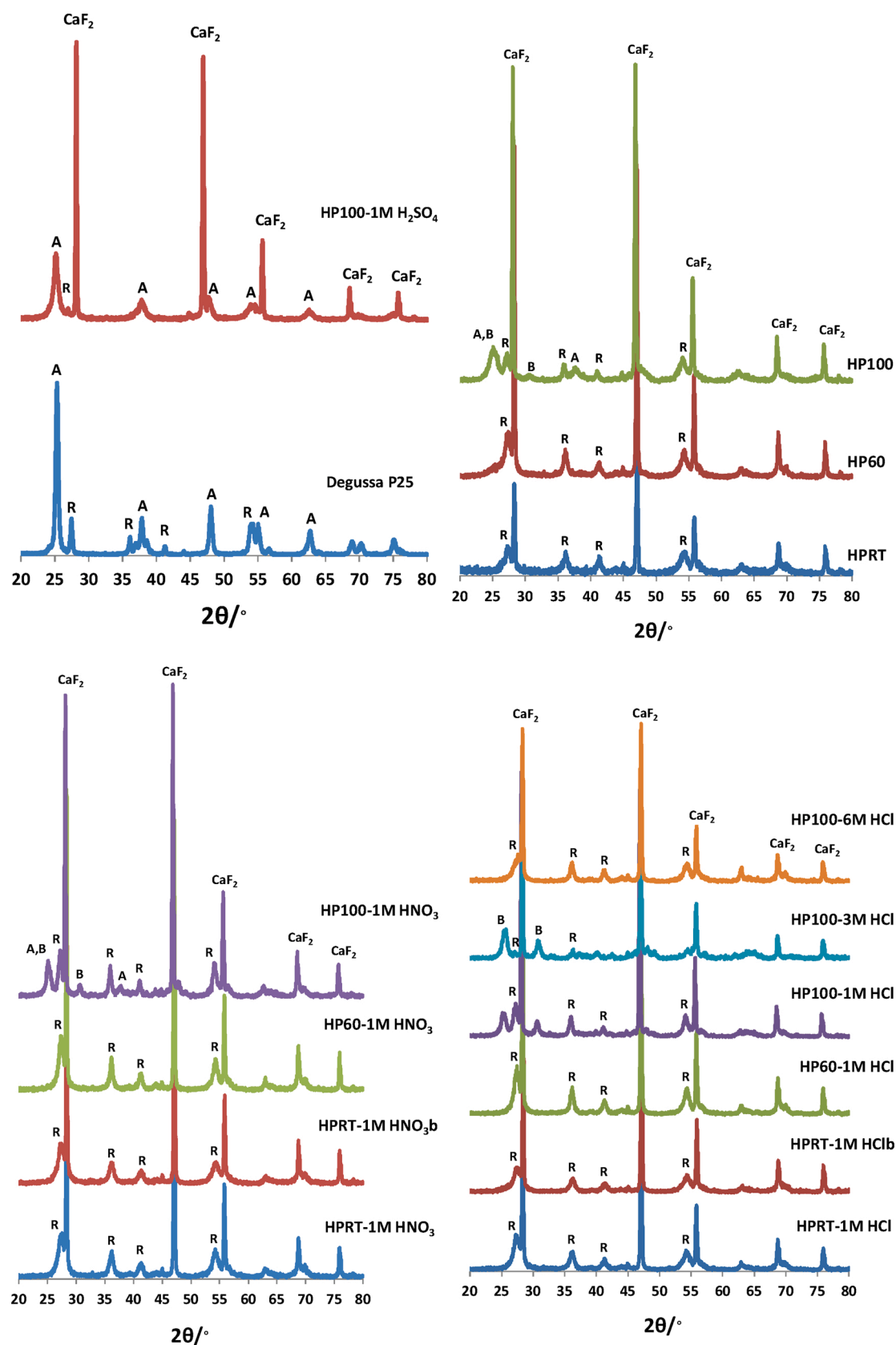


Fig. 1. XRD patterns of TiO₂ samples (Home prepared and Degussa P25) obtained with CaF₂ (50 %, w/w).

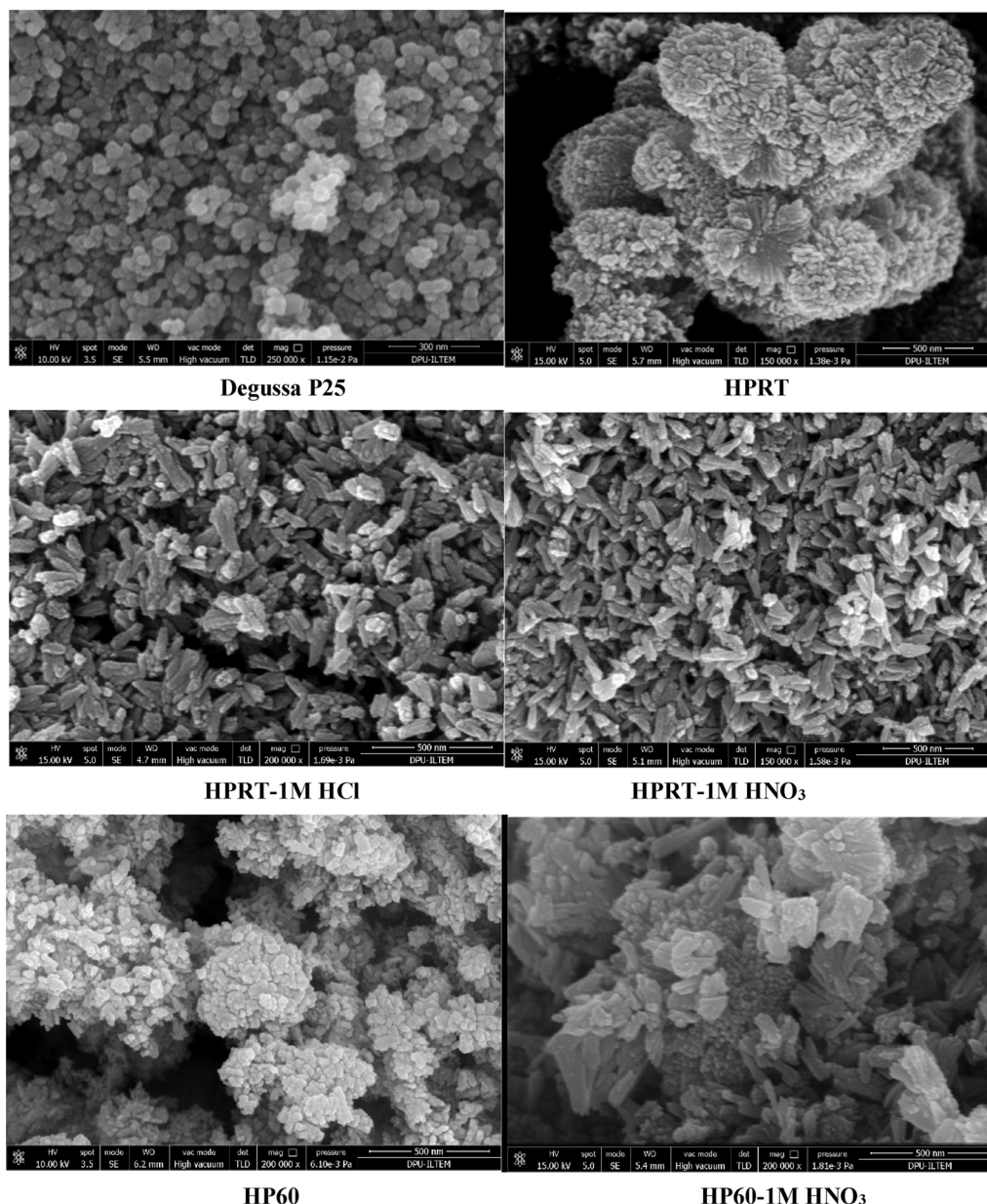


Fig. 2. SEM photos of home prepared and Degussa P25 TiO₂ samples.

P25 TiO₂ catalysts. The agglomerate size values of the TiO₂ nanoparticles were estimated from SEM images and reported in Table 1. The samples prepared without using an acid (HPRT, HP60 and HP100) have a similar spherical shape (particle size: ca. 30 nm), while other samples prepared at RT and 60 °C were nanorod shaped (ca. 25–200 nm, Width-Length). These results showed that the presence of acids and the used low temperatures for aging were beneficial for the formation of nanorods and of the rutile phase. Contrary, all of the samples presented spherical shape with about 30 nm of diameter at 100 °C of aging temperature. The image of HP100-6 M HCl catalyst indicated the presence of big agglomerates of TiO₂ particle, responsible of both the low surface area and pore volume that were determined.

Figs. 3–6 show TGA curves of TiO₂ photocatalysts. The curves could be divided in three regions [35]. The region between 30 and 120 °C indicate the physically adsorbed water (H₂O_{phys}) on the TiO₂ surface; the regions between 120 and 300 °C and between 300 and 500 °C indicate the weakly (OH_{weak}) and strongly (OH_{strong}) bonded hydroxyl groups on the TiO₂ surface, respectively. Table 2 reports these values

evaluated from the TGA curves as percentages. As the TiO₂ phase transitions also occurs at high temperature (i.e 400 °C), it is better to use H₂O_{phys} and OH_{weak} values rather than the OH_{strong} ones for comparison. All the TiO₂ samples prepared at low or moderate temperature have H₂O_{phys} and OH_{weak} values very higher than commercial Degussa P25. For instance, H₂O_{phys} and OH_{weak} values of HP100-1 M H₂SO₄ were ca. 5 and 4 times higher, respectively. These results showed that our samples were more hydrophilic than Degussa P25. Moreover, by increasing the preparation temperature, from RT to 100 °C, both H₂O_{phys} and OH_{weak} values decreased for the samples prepared by using the same starting solution (i.e. see Figs. 3 and 4). In addition, the mass loss indicated also the transition from the amorphous to crystalline phase; high mass loss values were determined for the poorly crystalline, and mainly amorphous home prepared samples. As discussed above, the mass loss values for HP100-6 M HCl were smaller than those found for the other home prepared samples. Nevertheless, to justify and to compare straightforwardly the figures of all of the home prepared samples was difficult, due to the different BET specific surface areas of the solids.

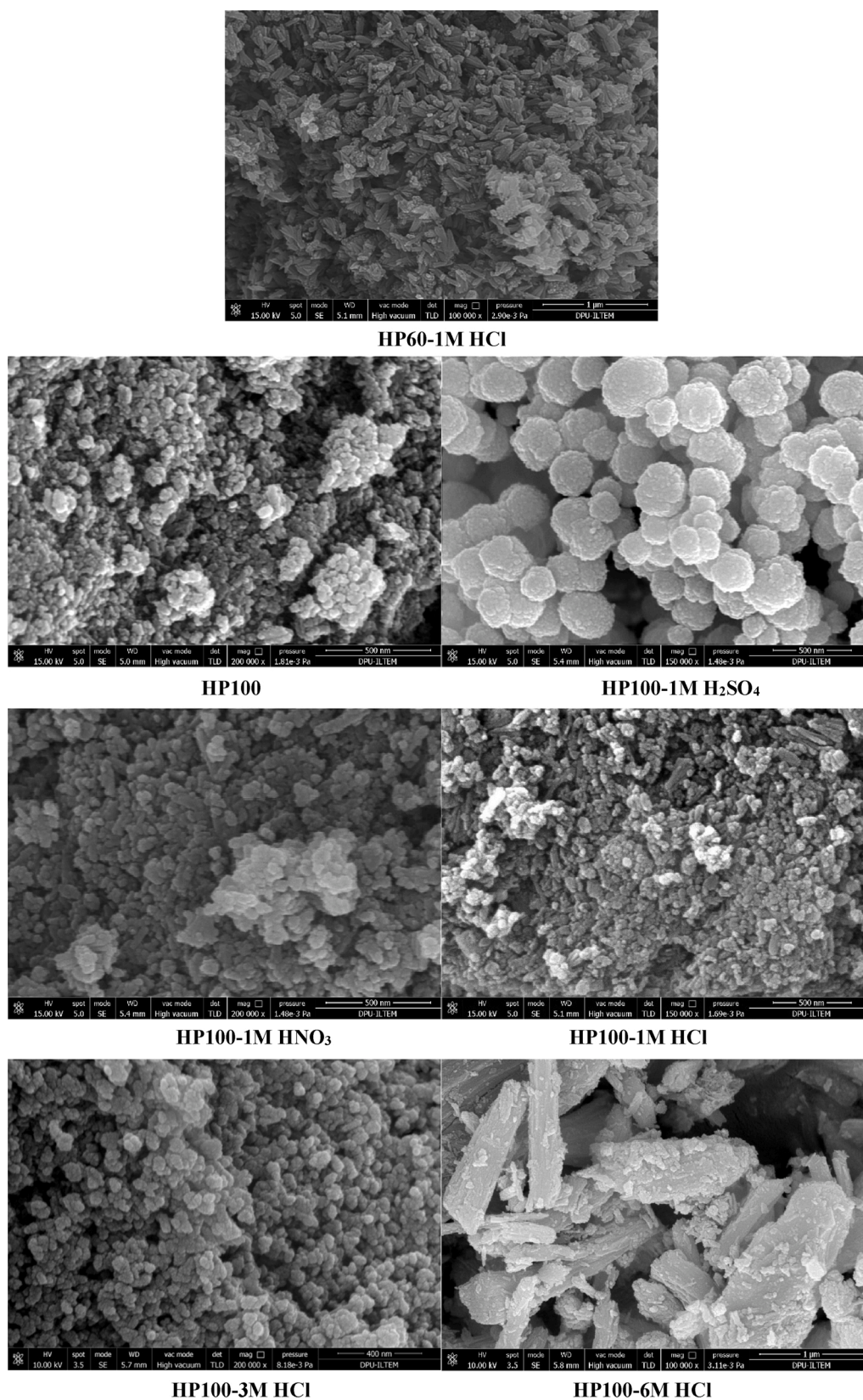


Fig. 2. (continued).

3.2. Photocatalytic activity

Fig. 7 shows the photocatalytic oxidation of 3-pyridinemethanol to 3-pyridinemethanal and vitamin B₃ versus time by aqueous suspension

of HPRT-1 M HNO₃ catalyst at pH 7 under UVA irradiation. The first and second oxidation products of 3-pyridinemethanol were 3-pyridinemethanal and vitamin B₃, respectively. For this reason, the 3-pyridinemethanal concentration increased like a Langmuir curve due to its

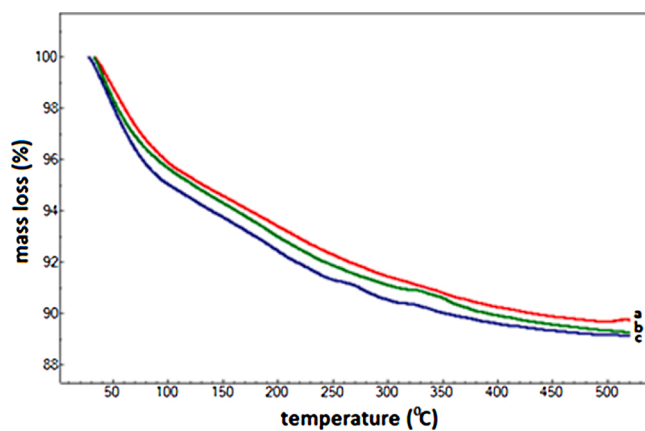


Fig. 3. TGA curves of HP100 (a), HP60 (b) and HPRT (c).

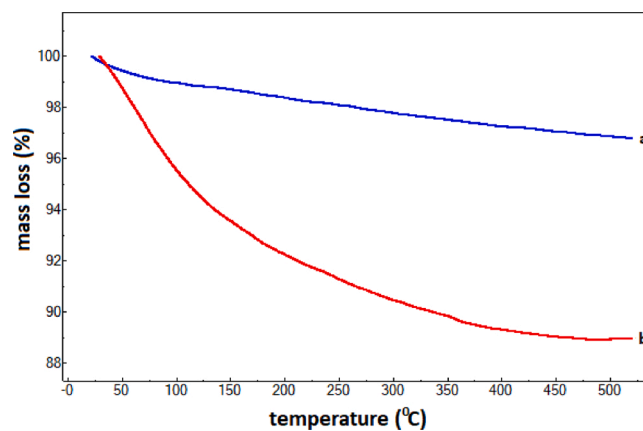


Fig. 6. TGA curves of Degussa P25 (a) and HP100-1 M H₂SO₄ (b).

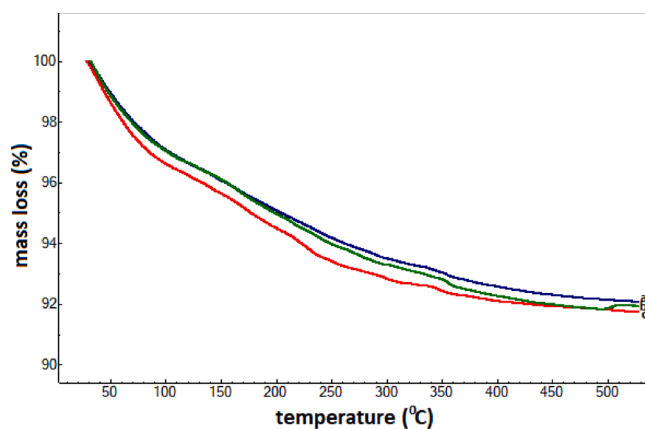


Fig. 4. TGA curves of HP100-1 M HNO₃ (a), HP60-1 M HNO₃ (b) and HPRT-1 M HNO₃ (c).

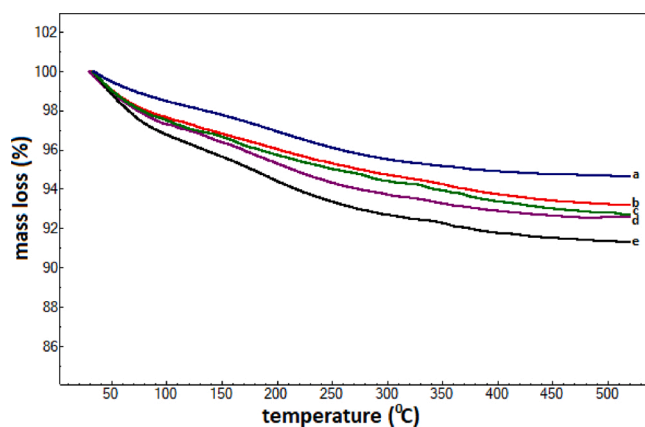


Fig. 5. TGA curves of HP100-6 M HCl (a), HP100-1 M HCl (b), HP100-3 M HCl (c), HP60-1 M HCl (d) and HPRT-1 M HCl (e).

further oxidation to vitamin B₃ throughout the reaction. On the contrary, vitamin B₃ concentration increased continuously at least for 3 h. These results overlapped with the selectivity results; the aldehyde selectivity decreased from ca. 80 to 44 %, while that of the acid increased from ca. 11–23% from the initial to the end of the reaction (3 h). After 3 h of reaction time, the sum of the selectivity towards the aldehyde, the acid and mineralized CO₂ (divided by 6 for stoichiometric normalization) was 80 %, and the carbon balance was not achieved, due to the presence of unknown over-oxidation aliphatic species that

Table 2

The mass percentage values of physically adsorbed water (H₂O_{phys}), weakly (OH_{weak}) and strongly bonded hydroxyl (OH_{strong}) groups evaluated from TGA curves. OH_{total} = OH_{weak} + OH_{strong}.

Catalyst	H ₂ O _{phys} [30–120 °C] (%)	OH _{weak} [120–300 °C] (%)	OH _{strong} [300–500 °C] (%)	OH _{total} [120–500 °C] (%)
Degussa P25	0.972	1.05	0.940	1.99
HPRT	5.38	4.04	1.34	5.38
HPRT-1 M HCl	3.69	3.63	1.33	4.96
HPRT-1 M HNO ₃	3.68	3.42	1.03	4.45
HP60	5.08	3.99	1.78	5.77
HP60–1 M HCl	2.98	3.25	1.13	4.38
HP60–1 M HNO ₃	3.36	3.37	1.43	4.80
HP100	4.67	3.38	1.77	5.15
HP100–1 M HCl	2.70	2.59	1.50	4.09
HP100–3 M HCl	2.94	2.67	1.59	4.26
HP100–6 M HCl	1.83	2.67	0.838	3.51
HP100–1 M HNO ₃	3.36	3.15	1.37	4.52
HP100–1 M H ₂ SO ₄	5.28	4.16	1.60	5.76

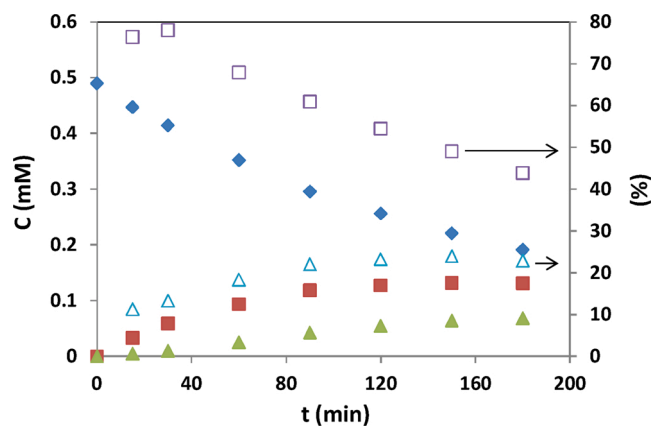


Fig. 7. Results of photocatalytic oxidation of 3-pyridinemethanol (◆) to 3-pyridinemethanal (■) and vitamin B₃ (▲) versus time in the presence of HPRT-1 M HNO₃ at pH 7 under UVA irradiation. The 3-pyridinemethanal (□) and vitamin B₃ (Δ) selectivity's were shown in the right ordinate.

Table 3Photocatalytic oxidation results of 3-pyridinemethanol (0.5 mM) to 3-pyridinemethanal and vitamin B₃ at pH 7 under UVA irradiation.

Catalyst	$-r_0 \times 10^3$ (mM h ⁻¹)	$k \times 10^3$ (h ⁻¹)	^a S _{3-Pyridinemethanal} (%)			^b S _{Vitamin B₃} (%)			^c S _{CO₂/6 X_{3h}} (%)	X _{1h} (%)	X _{3h} (%)	C-balance X _{0.50} (%)
			X _{0.15}	X _{0.30}	X _{0.50}	X _{0.15}	X _{0.30}	X _{0.50}				
Degussa P25	328	582	40	38	35	9	8	11		52	83	
HPRT	110	324	76	69	57	16	19	26		27	61	
HPRT-1 M HCl	163	261	74	64	52	14	19	23	5.1	28	55	80
HPRT-1 M HClb	177	292	80	73	57	13	18	24	15	30	59	
HPRT-1 M HNO ₃	151	324	78	67	53	13	19	24	21	28	61	
HPRT-1 M HNO ₃ b	181	283	82	71	57	14	21	23	8.4	31	58	
HP60	101	219	79	70	60	12	18	23	1.1	20	48	84
HP60-1 M HCl	120	258	78	67	52	14	19	23	13	24	54	88
HP60-1 M HNO ₃	86	164	80	69		14	20		3.8	17	39	
HP100	136	294	71	61	53	10	12	17	24	29	58	
HP100-1 M HCl	104	240	66	57	50	11	14	19	14	24	52	83
HP100-3 M HCl	142	247	74	68	61	9	13	18	3.6	25	53	83
HP100-6 M HCl	3.7	7.5								0.7	2	
HP100-1 M HNO ₃	118	249	64	55	49	10	13	18	13	25	53	80
HP100-1 M H ₂ SO ₄	135	189	78	70		10	15		16	23	44	

$-r_0$: initial reaction rate, k : pseudo-first order rate constant, ^aS_{3-Pyridinemethanal} and ^bS_{Vitamin B₃}: 3-pyridinemethanal and vitamin B₃ selectivity's after 15 % (X_{0.15}), 30 % (X_{0.30}) and 50 % (X_{0.50}) conversions. X_{1h} and X_{3h}: conversion values after 1 h and 3 h of reaction, respectively. ^cS_{CO₂}: CO₂ selectivity after 3 h of reaction (X_{3h}).

Table 4Photocatalytic oxidation results of 3-picoline (0.5 mM) to 3-pyridinemethanol, 3-pyridinemethanal and vitamin B₃ at pH 7 under UVA irradiation.

Catalyst	$-r_0 \times 10^3$ (mM h ⁻¹)	$k \times 10^3$ (h ⁻¹)	^a S _{3-Pyridinemethanol} (%)			^b S _{3-Pyridinemethanal} (%)			^c S _{Vitamin B₃} (%)			^d S _{CO₂/6 X_{3h}} (%)	X _{1h} (%)	X _{3h} (%)	C-balance X _{0.50} (%)
			X _{0.15}	X _{0.30}	X _{0.50}	X _{0.15}	X _{0.30}	X _{0.50}	X _{0.15}	X _{0.30}	X _{0.50}				
Degussa P25	418	695		1.1	1.1		5.0	5.5		3.5	4.4	60	54	88	
HPRT	125	176	0.7	0.67			9.6	5.6		7.5	12	70	18	40	
HPRT-1 M HCl	123	143	0.3	0.58			3.5	4.1		1.6	2.5	72	16	36	
HPRT-1 M HNO ₃	117	120	0.5	0.55			3.6	4.3		0.95	2.2	75	16	32	
HP-60	104	144	0.6	0.77			5.6	5.6		1.9	2.4	64	15	36	
HP60-1 M HCl	139	184	0.5	0.58			6.6	5.7		3.5	4.7	61	19	44	
HP60-1 M HNO ₃	157	167	0.4	0.61			4	5.1		1.4	3.8	57	21	42	
HP100	161	251	0.9	1.2	1.0	6	8.5	7.8	1.9	3.5	4.1	46	22	54	59
HP100-1 M HCl	189	245	0.3	0.78	0.9	2.1	5.3	5.3	0.9	2.3	3.2	45	26	53	54
HP100-3 M HCl	249	347	0.8	1.9	2.0	4	7.5	8.7	0.7	2.4	4.9	39	36	66	
HP100-6 M HCl	116	96.5	0	0		0	0		0	0		89	13	28	
HP100-1 M HNO ₃	189	255	0.3	0.73	0.67	2	5.3	5.5	0.2	2.1	2.2	47	26	55	55
HP100-1 M H ₂ SO ₄	163	202	1.6	2.0	1.8	7.2	7.5	6.9	2.0	3	2.9	53	23	47	65

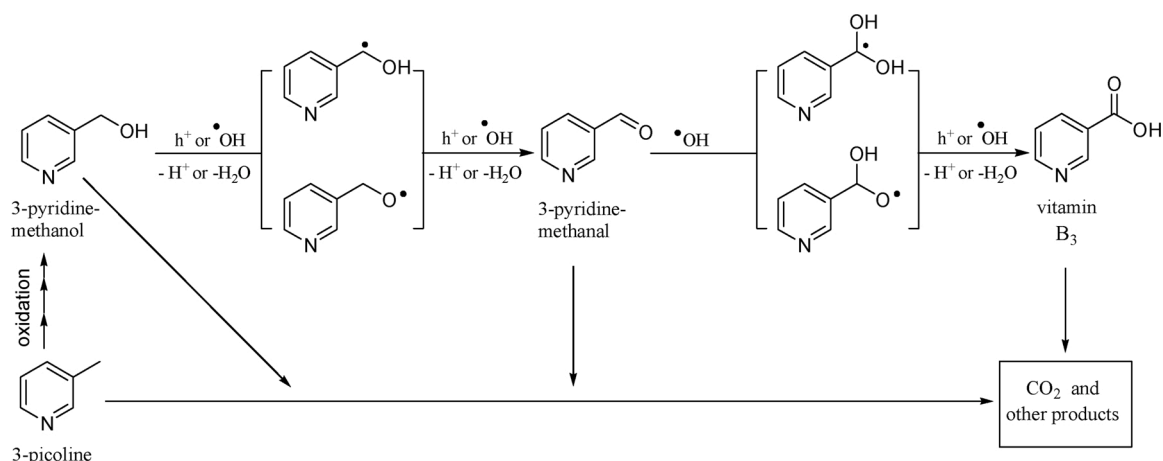
$-r_0$: initial reaction rate, k : pseudo-first order rate constant, ^aS_{3-Pyridinemethanol}, ^bS_{3-Pyridinemethanal} and ^cS_{Vitamin B₃}: 3-pyridinemethanol, 3-pyridinemethanal and vitamin B₃ selectivity's after 15 % (X_{0.15}), 30 % (X_{0.30}), and 50 % (X_{0.50}) conversions. X_{1h} and X_{3h}: conversion values after 1 h and 3 h of reaction, respectively. ^dS_{CO₂}: CO₂ selectivity after 3 h of reaction (X_{3h}).

probably derived from the breakdown of aromatic rings.

Table 3 shows selective photocatalytic oxidation results of 3-pyridinemethanol to 3-pyridinemethanal and vitamin B₃ at pH 7 under UVA irradiation. The initial reaction rate ($-r_0$) and pseudo-first order rate constant (k) values were reported in the Table. In addition, the values of 3-pyridinemethanal and vitamin B₃ selectivity's for 15, 30 and 50 % conversions and the conversion values after 1 and 3 h were also reported. The CO₂ selectivity values were given after 3 h of irradiation time. Degussa P25 showed the highest photocatalytic activity ($k = 0.583$ h⁻¹) for 3-pyridinemethanol oxidation, probably due to its good crystalline structure and to the synergic effect of the presence of both anatase and rutile phases. Among the home prepared catalysts, HPRT and HPRT-1 M HNO₃ ($k = 0.324$ h⁻¹) showed the highest activity by considering the k values. The prevalent phase of these two samples, prepared at room temperature, was the rutile one. The least photoactive sample, as expected, was the HP100-6 M HCl catalyst, and this can be mainly due to the very low value of its specific surface area. All home

prepared TiO₂ samples showed higher product selectivity than that of Degussa P25. As determined from TGA results, the TiO₂ surface of home prepared samples presented a high hydroxyl group density which allowed desorption of the produced valuable products without their over-oxidation. Consequently, the hydrophilic behaviour of TiO₂ surface was the reason of the high selectivity results. Generally, total 3-pyridinemethanal and vitamin B₃ selectivity values of home prepared catalysts were higher than 90 % after 15 % conversion, while it was only ca. 49 % for Degussa P25. As the over-oxidation of the produced products increases by increasing the reaction time, the total selectivity values decrease by increasing the conversion. C-balance (%) values were calculated for selected runs by considering the un-reacted 3-pyridinemethanol, the produced 3-pyridinemethanal, vitamin B₃, and CO₂ (divided by 6 for stoichiometric normalization) deriving from mineralization after 50 % conversion (see Table 3). Quite high C-balance values (80–88 %) were obtained by using home prepared TiO₂ catalysts.

Table 4 shows selective photocatalytic oxidation results of 3-picoline



Scheme 1. The proposed mechanism for photocatalytic oxidations of 3-picoline and 3-pyridinemethanol.

Table 5
Photocatalytic oxidation results of 3-picoline (0.5 mM) to 3-pyridinemethanol, 3-pyridinemethanal and vitamin B₃ under UVA irradiation at different pH's.

Catalyst	pH	$-r_0 \times 10^3$ (mM h ⁻¹)	$k \times 10^3$ (h ⁻¹)	^a S _{3-Pyridinemethanol} (%)			^b S _{3-Pyridinemethanal} (%)			^c S _{Vitamin B₃} (%)			^d S _{CO₂/6 X_{3h}} (%)	X _{1h} (%)	X _{3h} (%)
				X _{0.15}	X _{0.30}	X _{0.50}	X _{0.15}	X _{0.30}	X _{0.50}	X _{0.15}	X _{0.30}	X _{0.50}			
Degussa P25	1.98 ^e	35.3	46.3	5.5			49			15			low	5	14
Degussa P25	4.15	166	212	4.5	4.4	2.8	9.4	12	9.0	1.9	2	1.6	63	24	49
Degussa P25	7.0	418	695		1.1	1.1		5	5.5		3.5	4.4	60	54	88
Degussa P25	10	429	1188		0.86	0.93		4	5		2.7	4.3	52	62	98
Degussa P25	12.7 ^f	332	711		5.3	4.4		4.4	4.5		17	18	36	52	89
HP100-3 M HCl	2.08 ^e	35.0	26.1	6			53			13			low	4	8
HP100-3 M HCl	4.13	29.6	27.7	6			14			2			low	4	8
HP100-3 M HCl	7.0	249	347	0.8	1.9	2	4	7.5	8.7	0.7	2.4	4.9	39	36	66
HP100-3 M HCl	10.3	231	435	0.9	1.3	1.5	2.4	5.6	6.3	1.4	2.6	4	41	35	74
HP100-3 M HCl	12.7 ^f	189	305	5	5	3.6	2.5	4.0	3.8	12	16	14	45	29	60

$-r_0$: initial reaction rate, k : pseudo-first order rate constant, ^aS_{3-Pyridinemethanol}, ^bS_{3-Pyridinemethanal} and ^cS_{Vitamin B₃}: 3-pyridinemethanol, 3-pyridinemethanal and vitamin B₃ selectivity's after 15 % (X_{0.15}), 30 % (X_{0.30}), and 50 % (X_{0.50}) conversions. X_{1h} and X_{3h}: conversion values after 1 h and 3 h of reaction, respectively. ^dCO₂ selectivity's were considered after 3 h of reaction (X_{3h}). ^e[H₃O⁺] = 0.01 M; ^f[OH⁻] = 0.01 M.

to 3-pyridinemethanol, 3-pyridinemethanal and vitamin B₃. By starting from 3-picoline as the substrate, very low selectivity values were obtained with respect to those of 3-pyridinemethanol oxidation. Probably, the low selectivity's were due to preferential oxidation pathway of 3-picoline to CO₂ rather than to the corresponding alcohol, aldehyde or acid derivatives. Indeed, CO₂ selectivity values of 3-picoline substrate were very high (47–89 %) with respect to those of 3-pyridinemethanol (1–21 %) oxidation. The oxidation of methyl group of the aromatic ring of 3-picoline is more difficult with respect to that of the benzyl group [64]. The highest activity among home prepared samples appeared to be that of HP100-3 M HCl ($k = 0.347$ h⁻¹) which showed also the highest total product selectivity (ca. 16 %, without considering CO₂ selectivity) after 50 % conversion. This total product selectivity value was just ca. 11 % for Degussa P25. However, Degussa P25 showed the highest activity for 3-picoline oxidation reaction ($k = 0.695$ h⁻¹). HP100-6 M HCl showed almost no activity for 3-pyridinemethanol, while interestingly moderate activity for 3-picoline oxidation; 2 vs 28 % conversion after 3 h irradiation. Nevertheless, HP100-6 M HCl catalyst was the worst one with respect to the other catalysts for the conversion of both substrates and also for products selectivity. Virtually no products were obtained with the exception of CO₂ deriving from mineralization for which the highest value of ca. 89 % was found. C-balance (%) values for 3-picoline oxidation were also calculated for

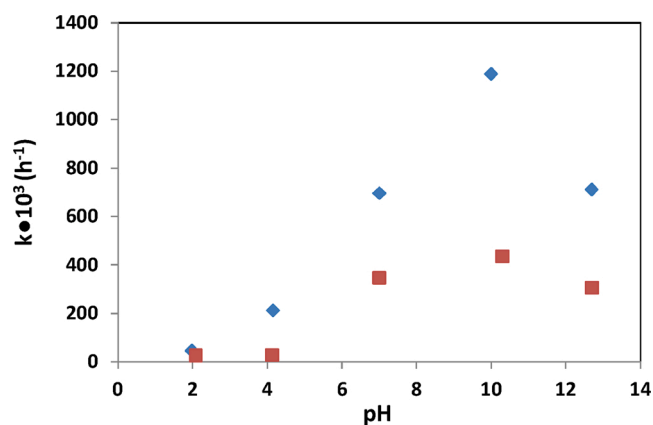


Fig. 8. k values of the photocatalytic oxidation of 3-picoline experiments by using Degussa P25 (◆) and HP100-3 M HCl (■) photocatalysts at different pH's.

selected runs by considering the un-reacted 3-picoline, the produced 3-pyridinemethanol, 3-pyridinemethanal, vitamin B₃, and CO₂ deriving from mineralization after 50 % conversion. Low C-balance values (54–65 %) were obtained by using TiO₂ catalysts as results of low selective oxidation of 3-picoline oxidation (see Table 4).

Scheme 1 shows a proposed mechanism for photocatalytic oxidation starting from 3-picoline or 3-pyridinemethanol. The first step of 3-picoline oxidation is the formation of 3-pyridinemethanol, but the mineralization pathway is preferred, as it can be noticed in Table 4. The further oxidation steps, after formation of 3-pyridinemethanol could be the interaction of h⁺ or hydroxyl radicals with formation of 3-pyridinemethanal subsequently oxidized to vitamin B₃. The over-oxidation products of these substrates and their corresponding molecules were mainly aliphatic species and CO₂.

3-Picoline oxidation was also performed at different pH values (ca. 2–12) by using HP100-3 M HCl and Degussa P25 photocatalysts, and the obtained results were reported in Table 5. Fig. 8 shows k values versus pH for 3-picoline oxidation. Very low activity values were obtained in acidic conditions, whereas the catalysts showed high activity in neutral and basic conditions (especially at pH 10). The highest total selectivity values were obtained at pH 2; HP100-3 M HCl and Degussa P25 show 72 and 70 % total selectivity (3-pyridinemethanol, 3-pyridinemethanal and vitamin B₃) respectively, after 15 % conversion. For this reason, CO₂ selectivity's were high in neutral and basic conditions, while CO₂ selectivity was negligible in acidic medium. In acidic condition the protonated aromatic ring of 3-picoline is more stable [64], and it could justify the resistance to a complete oxidation and the high product selectivity.

4. Conclusions

In this work TiO₂ samples were tested for selective photocatalytic oxidation of 3-pyridinemethanol and 3-picoline in aqueous suspension under UVA irradiation. The influence of the preparation experimental conditions (i.e. type of acid and temperature) on TiO₂ crystallinity, morphology and specific surface area was also investigated. The presence of acids in the preparation inhibited the TiO₂ formation, indeed in the presence of H₂SO₄ no TiO₂ was obtained at RT and 60 °C, and in the presence of 9 M HCl no TiO₂ was formed even at 100 °C. At low temperatures (RT and 60 °C) only rutile phase could be obtained, whilst at 100 °C in the presence of HCl and HNO₃ mainly brookite and rutile phases were found, and in the presence of H₂SO₄ mainly anatase phase was produced. Nanorod structured TiO₂ was formed in the presence of HCl or HNO₃ at RT and 60 °C. TiO₂ sample prepared in 6 M HCl (HP100-6 M HCl) resulted to have a very low BET surface area and consequently a very low activity. However, interestingly HP100-6 M HCl was much more active for 3-picoline oxidation than for 3-pyridinemethanol. Moreover, no valuable product was obtained with HP100-6 M HCl. All home prepared samples, with the exception of HP100-6 M HCl, were poorly crystalline and presented high BET specific surface area values. The product selectivity results of 3-pyridinemethanol oxidation were much higher than those of 3-picoline. However, selective 3-picoline oxidation could be performed at low pH (ca. 2) with low activity. Home prepared samples showed higher selectivity but lower activity than Degussa P25 TiO₂, due to their amorphous and hydrophilic character. The TiO₂ surface of home prepared samples have high hydroxyl group density, therefore the produced valuable products could desorb easily without their over-oxidation.

Declaration of Competing Interest

The authors report no declarations of interest.

Acknowledgements

The authors thank the Scientific Research Project Council of Afyon

Kocatepe University (BAP project no: 18.KARIYER.295) for economic support. Eng. Hakan Şahin (Afyon Kocatepe Üniversitesi, Teknoloji Uygulama ve Araştırma Merkezi, Turkey) for the XRD and BET, and Eng. Mehmet Akkaş (Kütahya Dumlupınar Üniversitesi, İleri Teknolojiler Merkezi, Turkey) for the SEM analyses.

Appendix A. Supplementary data

Supplementary material related to this article can be found, in the online version, at doi:<https://doi.org/10.1016/j.cattod.2020.11.004>.

References

- [1] V. Augugliaro, M. Bellardita, V. Loddo, G. Palmisano, L. Palmisano, S. Yurdakal, *J. Photochem. Photobiol. C* 13 (2012) 224–245.
- [2] A.H. Mamaghani, F. Haghighat, C.-S. Lee, *Appl. Catal. B* 203 (2017) 247–269.
- [3] Z. Shayegan, C.-S. Lee, F. Haghighat, *Chem. Eng. J.* 334 (2018) 2408–2439.
- [4] P.A.K. Reddy, P.V.L. Reddy, E. Kwon, K.-H. Kim, T. Akter, S. Kalagara, *Environ. Int.* 91 (2016) 94–103.
- [5] M.R.D. Khaki, M.S. Shafeeyan, A.A.A. Raman, W.M.A.W. Daud, *J. Environ. Manage.* 198 (2017) 78–94.
- [6] X. Chen, S. Shen, L. Guo, S.S. Mao, *Chem. Rev.* 110 (2010) 6503–6570.
- [7] Q. Xiang, J. Yu, M. Jaroniec, *J. Am. Chem. Soc.* 134 (2012) 6575–6578.
- [8] K. Maeda, K. Domen, *J. Phys. Chem. Lett.* 1 (2010) 2655–2661.
- [9] G. Zhang, Z.-A. Lan, X. Wang, *Angew. Chem. Int. Ed.* 55 (2016) 15712–15727.
- [10] K.C. Christoforidis, P. Fornasiero, *ChemCatChem* 9 (2017) 1523–1544.
- [11] S.N. Habisreutinger, L. Schmidt-Mende, J.K. Stolarczyk, *Angew. Chem. Int. Ed.* 52 (2013) 7372–7408.
- [12] J. Yu, J. Low, W. Xiao, P. Zhou, M. Jaroniec, *J. Am. Chem. Soc.* 136 (2014) 8839–8842.
- [13] K. Wang, Q. Li, B. Liu, B. Cheng, W. Ho, J. Yu, *Appl. Catal. B* 176–177 (2015) 44–52.
- [14] H. Takeda, K. Koike, H. Inoue, O. Ishitani, *J. Am. Chem. Soc.* 130 (2008) 2023–2031.
- [15] D. Sun, Y. Fu, W. Liu, L. Ye, D. Wang, L. Yang, X. Fu, Z. Li, *Chem. Eur. J.* 19 (2013) 14279–14285.
- [16] Y. Zhang, Z.-R. Tang, X. Fu, Y.-J. Xu, *ACS Nano* 4 (2010) 7303–7314.
- [17] H. Zeghliou, N. Khellaf, H. Djelal, A. Amrane, M. Bouhelassa, *Chem. Eng. Commun.* 203 (2016) 1415–1431.
- [18] I.K. Konstantinou, T.A. Albanis, *Appl. Catal. B* 49 (2004) 1–14.
- [19] A.N. Rao, B. Sivasankar, V. Sadasivam, *J. Mol. Catal. A-Chem.* 306 (2009) 77–81.
- [20] V. Subramanian, P.V. Kamat, E.E. Wolf, *Ind. Eng. Chem. Res.* 42 (2003) 2131–2138.
- [21] S. Yurdakal, V. Loddo, G. Palmisano, V. Augugliaro, L. Palmisano, *Catal. Today* 143 (2009) 189–194.
- [22] S. Yurdakal, S. Çetinkaya, M.B. Şarlak, L. Özcan, V. Loddo, L. Palmisano, *Catal. Sci. Technol.* 10 (2020) 124–137.
- [23] L. Özcan, S. Yurdakal, V. Augugliaro, V. Loddo, S. Palmas, G. Palmisano, L. Palmisano, *Appl. Catal. B* 132–133 (2013) 535–542.
- [24] S. Xie, Q. Zhang, G. Liu, Y. Wang, *Chem. Commun.* 52 (2016) 35–59.
- [25] J. Yang, C. Chen, H. Ji, W. Ma, J. Zhao, *J. Phys. Chem. B* 109 (2005) 21900–21907.
- [26] Y. Liu, J. Li, B. Zhou, S. Lv, X. Li, H. Chen, Q. Chen, W. Cai, *Appl. Catal. B* 111–112 (2012) 485–491.
- [27] F. Parrino, V. Loddo, V. Augugliaro, G. Camera-Roda, G. Palmisano, L. Palmisano, S. Yurdakal, *Catal. Rev.* 61 (2019) 163–213.
- [28] L.-L. Tan, W.-J. Ong, S.-P. Chai, A.R. Mohamed, *Chem. Eng. J.* 308 (2017) 248–255.
- [29] S. Yurdakal, V. Loddo, G. Palmisano, V. Augugliaro, H. Berber, L. Palmisano, *Ind. Eng. Chem. Res.* 49 (2010) 6699–6708.
- [30] G. Camera Roda, F. Santarelli, V. Augugliaro, V. Loddo, G. Palmisano, L. Palmisano, S. Yurdakal, *Catal. Today* 161 (2011) 209–213.
- [31] A.E. Cassano, O.M. Alfano, *Catal. Today* 58 (2000) 167–197.
- [32] S.M. Rodríguez, J.B. Gálvez, M.I.M. Rubio, P.F. Ibáñez, D.A. Padilla, M.C. Pereira, J.F. Mendes, J.C. De Oliveira, *Sol. Energy* 77 (2004) 513–524.
- [33] V. Augugliaro, G. Camera-Roda, V. Loddo, G. Palmisano, L. Palmisano, J. Soria, S. Yurdakal, *J. Phys. Chem. Lett.* 6 (2015) 1968–1981.
- [34] J. Kou, C. Lu, J. Wang, Y. Chen, Z. Xu, R.S. Varma, *Chem. Rev.* 117 (2017) 1445–1514.
- [35] S. Yurdakal, Ş.Ö. Yanar, S. Çetinkaya, O. Alagöz, P. Yalçın, L. Özcan, *Appl. Catal. B* 202 (2017) 500–508.
- [36] N. Li, X. Lang, W. Ma, H. Ji, C. Chen, J. Zhao, *Chem. Commun.* 49 (2013) 5034–5036.
- [37] L. Palmisano, V. Augugliaro, M. Bellardita, A. Di Paola, E. García López, V. Loddo, G. Marci, G. Palmisano, S. Yurdakal, *ChemSusChem* 4 (2011) 1431–1438.
- [38] J.C. Colmenares, R. Luque, *Chem. Soc. Rev.* 43 (2014) 765–778.
- [39] J.C. Colmenares, Y.-J. Xu, *Heterogeneous Photocatalysis: From Fundamentals to Green Applications*, Springer-Verlag, Berlin Heidelberg, 2015. ISBN 978-3-662-48717-4.
- [40] J.C. Colmenares, Book chapter: nanophotocatalysis in selective transformations of lignocellulose-derived molecules: a Green approach for the synthesis of fuels, fine chemicals, and pharmaceuticals, in: N. Nuraje, R. Asmatulu, G. Mul (Eds.), Book Title: “Green Photo-Active Nanomaterials: Sustainable Energy and Environmental

- Remediation", The Royal Society of Chemistry, 2016, pp. 168–201. ISBN: 9781849739597.
- [41] X. Lang, X. Chen, J. Zhao, *Chem. Soc. Rev.* 43 (2014) 473–486.
- [42] K. Sivaranjani, C. Gopinath, *J. Mater. Chem.* 21 (2011) 2639–2647.
- [43] S. Yurdakal, B.S. Tek, O. Alagöz, V. Augugliaro, V. Loddo, G. Palmisano, L. Palmisano, *ACS Sust. Chem. Eng.* 1 (2013) 456–461.
- [44] I. Krivtsov, E.I. García-López, G. Marci, L. Palmisano, Z. Amghouz, J.R. García, S. Ordóñez, E. Díaz, *Appl. Catal. B* 204 (2017) 430–439.
- [45] M. Bellardita, V. Loddo, G. Palmisano, I. Pibiri, L. Palmisano, V. Augugliaro, *Appl. Catal. B* 144 (2014) 607–613.
- [46] C. Minero, A. Bedini, V. Maurino, *Appl. Catal. B* 128 (2012) 135–143.
- [47] V. Augugliaro, H.A.H. El Nazer, V. Loddo, A. Mele, G. Palmisano, L. Palmisano, S. Yurdakal, *Catal. Today* 151 (2010) 21–28.
- [48] Y. Zhang, N. Zhang, Z.-R. Tang, Y.-J. Xu, *Chem. Sci.* 4 (2013) 1820–1824.
- [49] D. Spasiano, R. Marotta, S. Malato, P. Fernandez-Ibañez, I. Di Sommaz, *Appl. Catal. B* 170–171 (2015) 90–123.
- [50] R. Chuck, *Appl. Catal. A* 280 (2005) 75–82.
- [51] K.G. Raghavan, B.M. Reddy, *Industrial Catalysis and Separations, Innovations for Process Intensification*, CRC Press, Oakville, Canada, 2015.
- [52] A. Martin, C. Janke, V.N. Kalevaru, *Appl. Catal. A* 376 (2010) 13–18.
- [53] D. Spasiano, L. Raspolini, S. Satyro, G. Mancini, F. Pirozzi, R. Marotta, *Chem. Eng. J.* 283 (2016) 1176–1186.
- [54] E.V. Ovchinnikova, T.V. Andrushkevich, G.Y.A. Popova, V.D. Meshcheryakov, V. A. Chumachenko, *Chem. Eng. J.* 154 (2009) 60–68.
- [55] Z. Song, T. Matsushita, T. Shishido, K. Takehira, *J. Catal.* 218 (2003) 32–41.
- [56] M. Alfe, D. Spasiano, V. Gargiulo, G. Vitiello, R. Di Capua, R. Marotta, *Appl. Catal. A* 487 (2014) 91–99.
- [57] T.R. Sobahi, M.S. Amin, *Appl. Nanosci.* 9 (2019) 1621–1636.
- [58] T. Ohno, T. Tsubota, R. Inaba, *J. Appl. Electrochem.* 35 (2005) 783–791.
- [59] M. Schiavello (Ed.), *Heterogeneous Photocatalysis*, Wiley, Chichester, 1997.
- [60] A. Fujishima, T.N. Rao, D.A. Tryk, *J. Photochem. Photobiol. C* 1 (2000) 1–21.
- [61] M. Bellardita, A. Di Paola, B. Megna, L. Palmisano, *J. Photochem. Photobiol. A* 367 (2018) 312–320.
- [62] M. Bellardita, A. Di Paola, B. Megna, L. Palmisano, *Appl. Catal. B* 201 (2017) 150–158.
- [63] S. Yurdakal, C. Garlisi, L. Özcan, M. Bellardita, G. Palmisano, Chapter title: (photo) catalyst characterization techniques: adsorption isotherms and BET, SEM, FTIR, UV-vis, photoluminescence, and electrochemical characterizations, in: G. Marci, L. Palmisano (Eds.), *Book Title: Heterogeneous Photocatalysis: Relationships With Heterogeneous Catalysis and Perspectives*, Elsevier, Netherlands, 2019, pp. 87–152. ISBN: 978-0-444-64015-4.
- [64] A. Katritzky, C.A. Ramsden, J. Joule, *Handbook of Heterocyclic Chemistry*, 3rd ed., Elsevier, Amsterdam, 2010.